

# Enhancing Colloidal Metallic Nanocatalysis: Sharp Edges and Corners for Solid Nanoparticles and Cage Effect for Hollow Ones

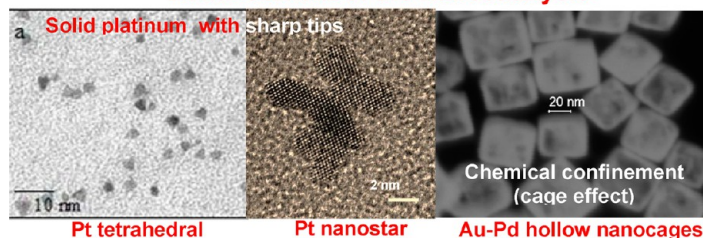
MAHMOUD A. MAHMOUD,<sup>§</sup> RADHA NARAYANAN,<sup>‡</sup> AND  
MOSTAFA A. EL-SAYED\*,<sup>§</sup>

<sup>§</sup>Laser Dynamics Laboratory, School of Chemistry and Biochemistry,  
Georgia Institute of Technology, Atlanta, Georgia 30332-0400, United States,  
and <sup>‡</sup>Department of Chemistry, University of Rhode Island, Kingston,  
Rhode Island 02881, United States

RECEIVED ON AUGUST 10, 2012

## CONSPECTUS

### Enhancement of the nanocatalysis



There are two main classes of metallic nanoparticles: solid and hollow. Each type can be synthesized in different shapes and structures. Practical use of these nanoparticles depends on the properties they acquire on the nanoscale. Plasmonic nanoparticles of silver and gold are the most studied, with applications in the fields of sensing, medicine, photonics, and catalysis. In this Account, we review our group's work to understand the catalytic properties of metallic nanoparticles of different shapes.

Our group was the first to synthesize colloidal metallic nanoparticles of different shapes and compare their catalytic activity in solution. We found that the most active among these were metallic nanoparticles having sharp edges, sharp corners, or rough surfaces. Thus, tetrahedral platinum nanoparticles are more active than spheres. We proposed this happens because sharper, rougher particles have more valency-unsatisfied surface atoms (i.e., atoms that do not have the complete number of bonds that they can chemically accommodate) to act as active sites than smoother nanoparticles. We have not yet resolved whether these catalytically active atoms act as catalytic centers on the surface of the nanoparticle (i.e., heterogeneous catalysis) or are dissolved by the solvent and perform the catalysis in solution (i.e., homogenous catalysis). The answer is probably that it depends on the system studied.

In the past few years, the galvanic replacement technique has allowed synthesis of hollow metallic nanoparticles, often called nanocages, including some with nested shells. Nanocage catalysts show strong catalytic activity. We describe several catalytic experiments that suggest the reactions occurred within the cage of the hollow nanocatalysts: (1) We synthesized two types of hollow nanocages with double shells, one with platinum around palladium and the other with palladium around platinum, and two single-shelled nanocages, one made of pure platinum and the other made of pure palladium. The kinetic parameters of each double-shelled catalyst were comparable to those of the single-shelled nanocage of the same metal as the inside shell, which suggests the reactions are taking place inside the cavity. (2) In the second set of experiments, we used double-shelled, hollow nanoparticles with a plasmonic outer gold surface and a non-plasmonic inner catalytic layer of platinum as catalysts. As the reaction proceeded and the dielectric function of the interior gold cavity changed, the plasmonic band of the interior gold shell shifted. This strongly suggested that the reaction had taken place in the nanocage. (3) Finally, we placed a catalyst on the inside walls of hollow nanocages and monitored the corresponding reaction over time. The reaction rate depended on the size and number of holes in the walls of the nanoparticles, strongly suggesting the confinement effect of a nanoreactor.

## 1. Introduction

Catalysis research using nanoparticles is a rapidly growing field driven by the progress in materials research.<sup>1,2</sup> The unique catalytic properties of nanocatalysts result from their size reduction and shape variation.<sup>3,4</sup> The reduction in size of the catalyst to the nanoscale causes at least two effects: (1) changing the electronic structure of metallic nanocatalysts, that is, increasing the Fermi level of the nanocatalyst leading to a lower reduction potential of the metal on the surface of the nanocatalyst,<sup>5</sup> and (2) increasing the number of chemically unsaturated and thermodynamically high-energy active surface atoms.<sup>3,4,6,7</sup> It has also been suggested that the type of exposed crystal planes, which can be controlled by the nanocatalyst shape, can influence the activity and selectivity of the nanocatalyst.<sup>8</sup> Moreover, some nanocatalysts acquire new properties such as plasmonic electromagnetic fields.<sup>9</sup>

Although catalysts of nanoscale dimensions possess advantages, problems that present a significant hindrance on the future applications of nanoparticles in catalysis result from the following: (1) reshaping of the nanocatalyst during catalysis reaction,<sup>3,10</sup> (2) products depositing on the nanocatalyst surface could decrease the nanoparticle stability and limit their recycling, (3) capping materials on the surface of colloidal nanocatalysts reduce their activity and can affect their Fermi energy,<sup>11</sup> and (4) aggregation of the nanocatalyst (especially in organic solvents).<sup>11</sup> Many efforts have been put forth to overcome these problems and improve the efficiency and selectivity of the nanocatalysts. These include (1) loading the nanocatalysts on a support (microscale materials, microgels, or zeolite support)<sup>12</sup> for improved stability and recyclability, (2) partially coating the surface with porous silica or a brush type polymer to improve the stability of the nanocatalysts in different media,<sup>13,14</sup> (3) cleaning the surface of nanocatalysts using oxygen plasma or UV irradiation, and (4) assembling the nanocatalyst on the surface of a substrate by Langmuir–Blodgett technique<sup>15</sup> or preparing it on the surface of a substrate by a lithographic technique.

An important question that arises in this field is whether catalysis using nanoparticles is heterogeneous<sup>16</sup> or homogeneous.<sup>6,17</sup> The common and acceptable definition of colloidal heterogeneous nanocatalysis is when the reaction occurs on the surface of nanoparticles. However in homogeneous catalysis, the solvent can dissolve high-energy atoms or ions from the sharp edges or corners of the nanoparticle surface and form a complex that can catalyze the reaction in solution.

Our group was the first to synthesize solid metallic (platinum) nanoparticles of different shapes<sup>2</sup> and suggested that this should have great effect in the field of nanocatalysis. We then studied the catalytic properties of colloidal nanoparticles of different shapes.<sup>3,10,6,7</sup> Recently, Sun and Xia<sup>18</sup> introduced the use of the galvanic replacement technique in making hollow gold nanoboxes from silver nanocubes. This very useful method has stimulated our group<sup>9,15,19–23</sup> and others<sup>24,25</sup> in using this method to develop the synthesis of the double shell hollow nanostructures.<sup>9,22,23</sup> This Account has two parts. In section 2, we discuss our contributions and conclusions to the field of nanocatalysis with solid nanoparticles of different shapes. In section 3, we discuss our synthesis and catalysis results of hollow nanoparticles with single and double shells. We will discuss the results of designed experiments that showed that catalysis with hollow nanoparticles occurs in the cavity.

## 2. Catalysis with Solid Metallic Nanoparticles

**2.1. Shape Dependence.** We studied the effect of nanoparticle shape on the catalytic activity for the electron transfer reaction between hexacyanoferrate(III) and thiosulfate ions to form hexacyanoferrate(II) and tetrathionate ions.<sup>3</sup> Three different shapes of platinum nanoparticles were investigated; tetrahedral, cubic, and spherical. The catalytic activity was found to be highly correlated to the fraction of atoms present at the corners and edges of the nanoparticles. Figure 1 illustrates the effect of three different shaped platinum nanoparticles on their activation energies. The tetrahedral platinum nanoparticles had the highest fraction of surface atoms on the corners and edges, as well as the highest catalytic activity with the lowest activation energy ( $14.0 \pm 0.6$  kJ/mol).<sup>3</sup> The cubic platinum nanoparticles had the lowest values of both the fraction of surface atoms on the corners and edges and the catalytic activity with the highest value of activation energy ( $26.4 \pm 1.2$  kJ/mol). The spherical platinum nanoparticles stand between showing intermediate fraction of surface atoms on the corners and edges and intermediate catalytic activity with intermediate activation energy ( $22.6 \pm 1.2$  kJ/mol).

Similar high catalytic activity was observed using a unique single-crystal multiarmed platinum nanostar with an average size of 11 nm.<sup>7</sup> This shape prepared by a seeded-growth mechanism from the tetrahedral platinum nanoparticles had multiple arms, up to 17 (see figure 2). The activation energy for the catalytic reduction of hexacyanoferrate(III) ions with thiosulfate ions was 14 kJ/mol when catalyzed by the platinum nanostar. This low value of

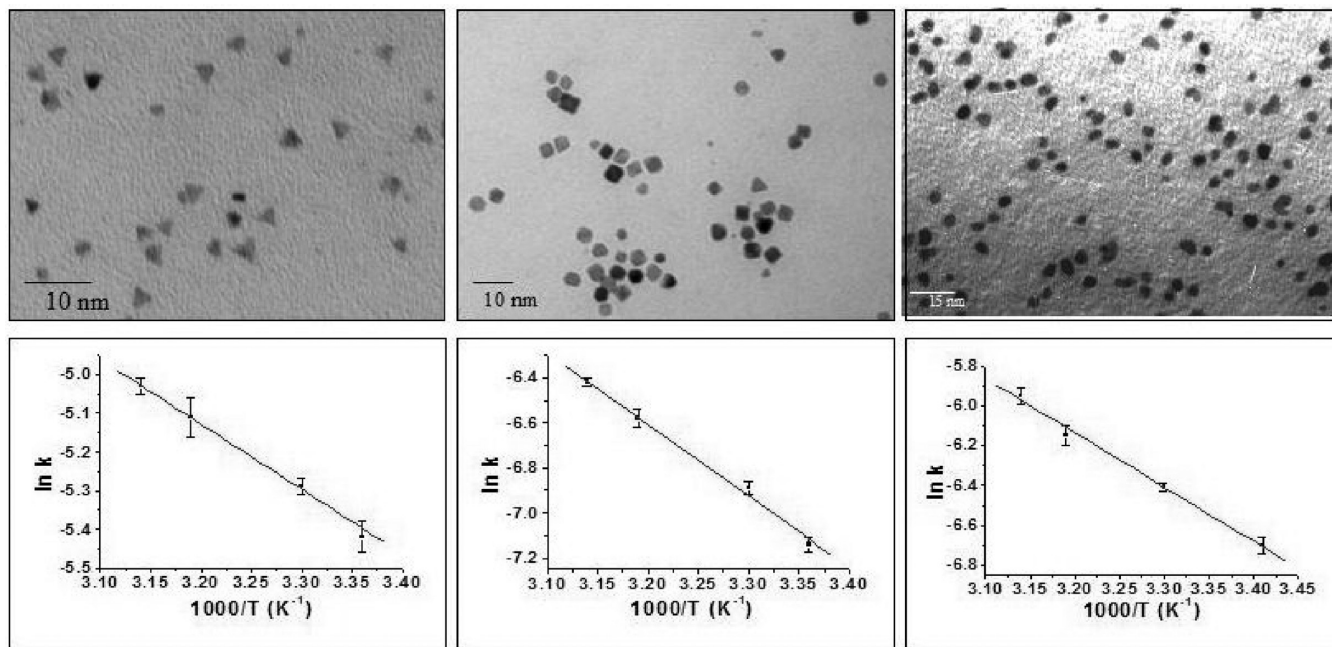


FIGURE 1. Effect of nanoparticle shape on the activation energies and catalytic activities of tetrahedral, cubic, and spherical platinum nanoparticles.<sup>3</sup>

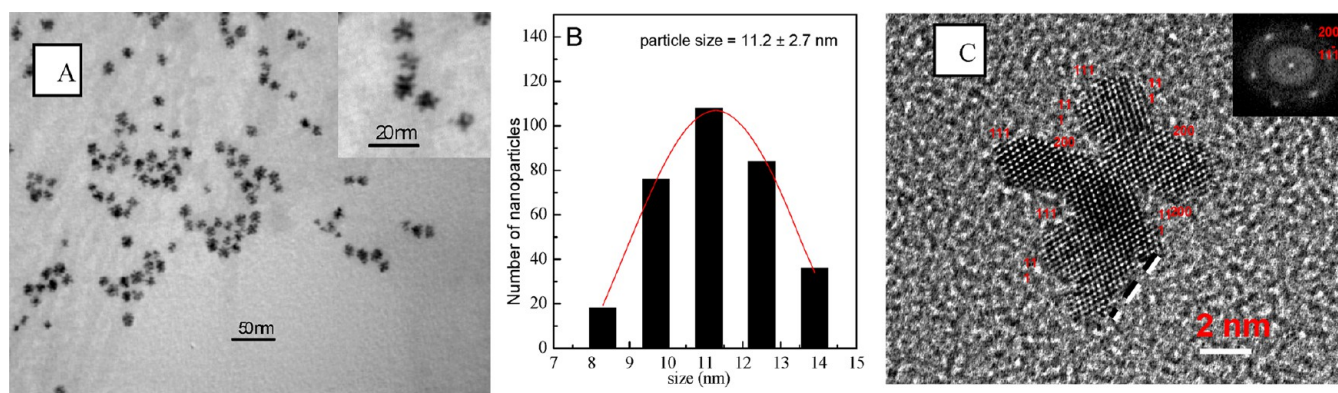


FIGURE 2. TEM image of platinum multiarmed nanostar<sup>8</sup> (A). The statistical size distribution curve for 300 particles taken from three different preparations using the same synthetic method (B). High-resolution TEM image of a single platinum nanostar (C), showing that the nanoparticle is a single crystal.<sup>7</sup>

activation energy was caused by the presence of many active edge and corner sites, as well as the presence of high index sites observed in the HRTEM images, of the nanostar structure.<sup>7</sup> More recently, Xia and his group have synthesized multioctahedral Pt nanocrystals, which showed a high catalytic performance.<sup>26</sup>

**2.2. Shape Changes of Solid Nanoparticle during Catalysis.** In order to determine the effect of the catalytic process on the nanoparticle shape, we monitored the nanoparticle shape as well as the activation energies at different times during the full course of the reaction.<sup>27</sup> As shown in Figure 3, it was found that both the tetrahedral and cubic platinum nanoparticles strive toward the most stable spherical shape,

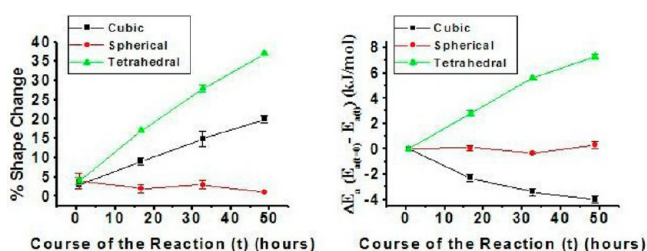
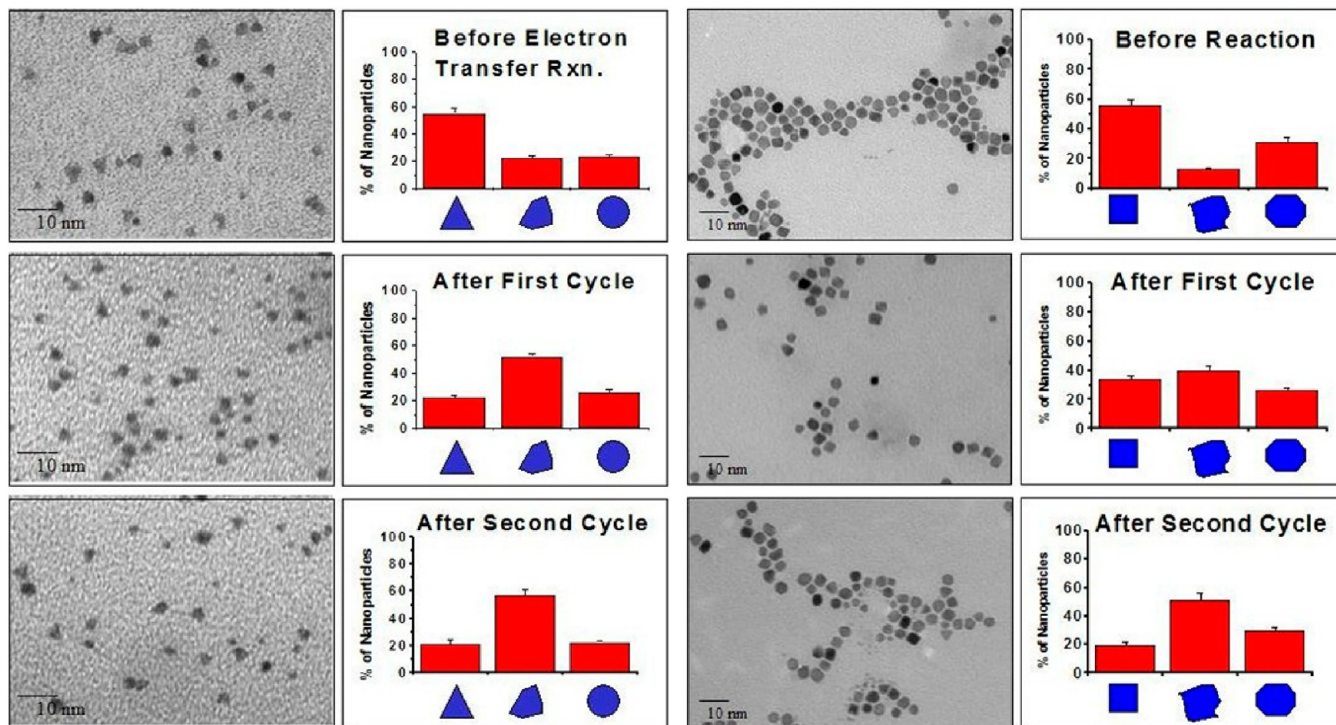


FIGURE 3. Amount of distortion in nanoparticle shape over time for the three shapes of nanoparticles and also the different changes in the value of the activation energy over time for the three shapes of nanoparticles.<sup>27</sup>

while there was minimal change in the spherical platinum nanoparticles.<sup>27</sup> In case of the tetrahedral platinum



**FIGURE 4.** Distortions in the shape of the tetrahedral and cubic platinum nanoparticles after the first and second cycles of the electron transfer reaction.<sup>17</sup>

nanoparticles, the activation energy increased during the course of the reaction and approaches that of the spherical platinum nanoparticles. On the other hand, the cubic platinum nanoparticles showed a decrease in the activation energy due to the creation of more sharp corners and edges and the transformation to spherical platinum nanoparticles.

Changes in shape taking place for both the tetrahedral and cubic platinum nanoparticles was also monitored after the first and second cycle of the electron transfer reaction. It was observed that the rate of shape change was faster for the tetrahedral platinum nanoparticles compared with the cubic platinum nanoparticles.<sup>17</sup> This can be seen in Figure 4, which compares the shape distribution of the tetrahedral and cubic nanoparticles after the first and second cycle of the electron transfer reaction. When tetrahedral platinum nanoparticles were used as catalysts for the electron transfer reaction, it was observed that there was a distortion of the shape that continued even after the first cycle of the reaction. In the case of the cubic platinum nanoparticles, the nanoparticle distortion occurred only after the first cycle of the electron transfer reaction.<sup>17</sup>

**2.3. Nanoparticles Used in the Catalysis of the Suzuki Reaction.** The first experiment in using nanoparticles in the catalysis of the Suzuki reaction was carried out in our laboratory.<sup>28</sup> The tetrahedral palladium nanoparticles have

been used as catalysts for two cycles of the Suzuki cross-coupling reaction between phenylboronic acid and iodobenzene to form biphenyl.<sup>4</sup> Figure 5 shows TEM images of the tetrahedral palladium nanoparticles after the first and second cycles of the Suzuki cross-coupling reaction. It was observed that after the first cycle of the reaction, the tetrahedral palladium nanoparticles were transformed into comparable size spherical palladium nanoparticles. This is most likely due to the relatively harsh conditions of the Suzuki reaction in which the reaction is conducted at high temperatures with long reflux times.<sup>4</sup> For spherical nanoparticles, it was observed that after the second cycle of the reaction, nanoparticles grew larger. This increase in size is attributed to the Ostwald ripening process in which there is a dissolution of the smaller nanoparticles having high surface energy and growth of the larger nanoparticles<sup>4</sup> whose surface has lower energy.

### 3. Catalysis with Hollow Nanoparticles: The Cage Effect

**3.1. Results Suggesting the Dominance of Cage Catalysis in Hollow Nanoparticles.** The kinetic parameters (rate constant of the reaction, activation energy, entropy of activation, and frequency factor) for a nanocatalytic reaction are controlled by following factors: the concentration of the

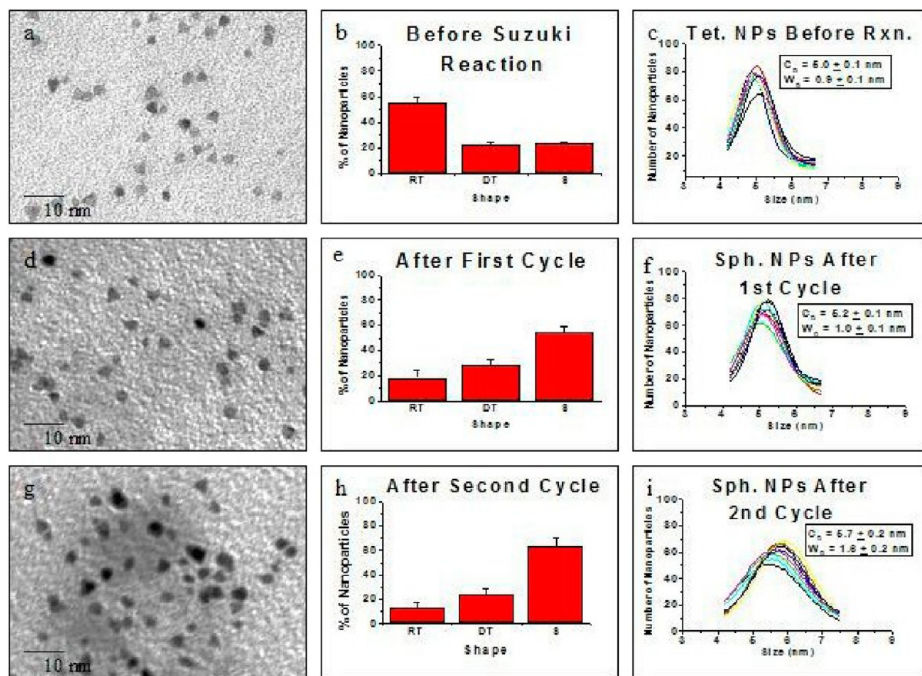


**FIGURE 5.** TEM images, shape distributions, and size distributions of the tetrahedral palladium nanoparticles after the first and second cycle of the Suzuki reaction.<sup>4</sup>

nanocatalyst and of the reacting materials, the number of successful collisions with the surface of the nanocatalyst in the rate-determining step, the Fermi energy of the nanocatalyst for a catalytic oxidation reaction, the shape of the nanocatalyst,<sup>3</sup> and the reaction temperature.

In nanocatalysis by solid nanoparticles, the catalytic reaction takes place only by involving the surface or atoms from the surface of the nanocatalyst, while the reaction for hollow nanocatalysts can take place by involving the outer or the inner surfaces of the nanocatalyst or both. Reactions in the hollow nanoparticle cavity could be assisted by several factors. First, the confinement effect of the cage could increase the steady-state concentration of the species in the rate-determining step of the reaction, and second, in some cases, the inner surface might not be as well capped as the outer surface and thus be more catalytically active.<sup>9</sup> Therefore, the rate of the reaction increases due to the confinement of the cage effect.<sup>24</sup> Since the wall thickness of the nanoreactor is small (few nanometers), the electron can transfer across the wall during catalysis of electron transfer reactions.<sup>29</sup> The surface to volume ratio of the hollow nanocatalyst is higher than any solid nanocatalyst, because the surface area of the cavity adds to the outer surface area of the nanocatalyst. This is another factor enhancing the catalytic properties of the hollow nanoparticles.

Porous metal–organic frameworks (MOFs) were prepared by Yaghi's group<sup>30</sup> and used in catalysis (catalyst or catalyst support) and in gas storage materials. The exciting applications of the MOF are based on their characteristic high surface area and voids in their structure.<sup>30</sup> Recently, hybrid inorganic nanocages made of ruthenium and  $\text{Cu}_2\text{S}$  were prepared and showed high electrocatalytic efficiency due to their high surface area and exciting electronic properties.<sup>24</sup> An unusually high efficiency of platinum and ruthenium nanocatalysts, prepared in situ inside polymer nanofibers, in the hydrogenation of organic compounds by hydrogen was observed.<sup>31</sup> This high activity is due to the cage effect. A nanoreactor made of nickel, cobalt, iron, and their oxides coated by  $\text{SiO}_2$  in a yolk–shell structure with nanosize space showed excellent catalytic performance and thermal stability.<sup>32</sup> Palladium nanotubes were used to catalyze Suzuki reaction with high efficiency.<sup>14</sup> Platinum cubic nanoboxes were found to have 1.5 times more activity than hollow Pt nanospheres for the same catalytic reaction.<sup>33</sup> Recently, Zeng et al.<sup>29</sup> compared the catalytic activity of gold nanocages, partially hollow nanoboxes, and solid nanocubes and found that Au nanocages exhibited the highest catalytic activity.<sup>29</sup>

Gold nanoparticles encapsulated in silica nanospheres showed a high catalytic performance for hydrogen generation from formic acid.<sup>34</sup> Moreover, nanoporous Pt nanoparticles

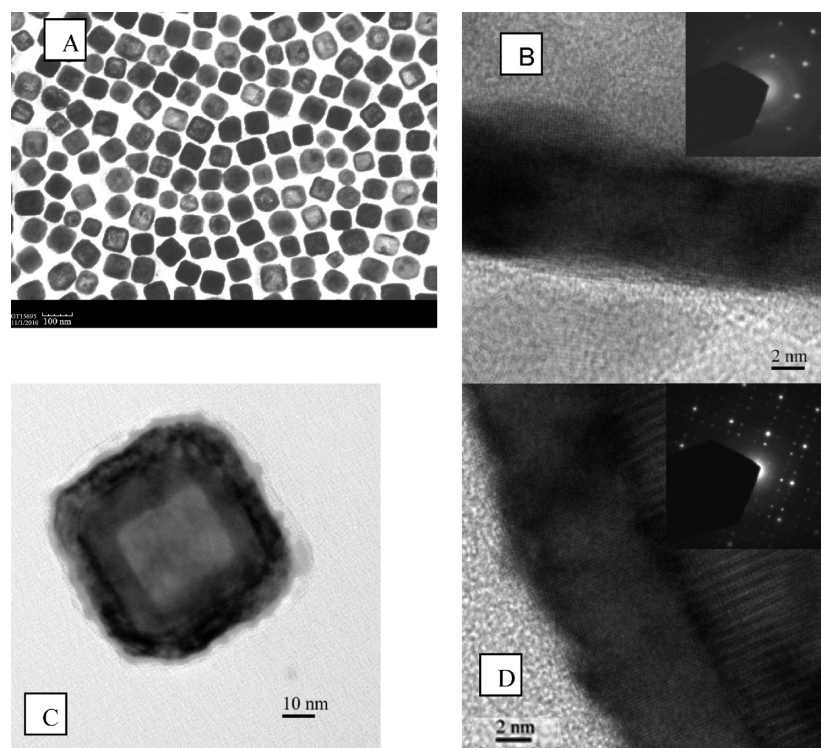


**FIGURE 6.** (A) TEM image of 89 nm PtNCs. (B) HR-TEM of PtNCs and the electron diffraction. (C) Magnified TEM image of a platinum–palladium shell–shell nanocage. (D) High-resolution TEM image of PtPdNCs; the inset is the diffraction pattern for the PtPdNCs. PtNCs have one diffraction pattern, while PtPdNCs have two patterns due to the presence of the two metals in the same nanoparticle. The high-resolution TEM image of PtPdNC in panel D shows three layers: pure Pt (outer), pure Pd (inner), and a middle Pt–Pd alloy layer. PtNCs in B has only one layer.

prepared by dealloying of Ni/Pt nanoparticle alloy showed good catalytic activity for the cathodic oxygen reduction reaction.<sup>35</sup> The catalytic efficiency of Pd–Pt alloy hollow nanoparticles is enhanced for oxygen reduction.<sup>36</sup> Density functional theoretical calculation proved a geometric effect on the catalytic properties; however, electronic confinement effects on catalysis were reported.<sup>37</sup>

**3.2. Different Designs of Hollow Nanocatalysts.** Different techniques have been used to synthesize hollow nanoparticles of different metals and composition, such as template (polymer beads or silica) mediated methods,<sup>38</sup> metal diffusion based on the Kirkendall effect,<sup>39</sup> and the galvanic replacement method.<sup>18</sup> The galvanic replacement method was used to synthesize many hollow nanoparticles.<sup>15,22,23</sup> This method utilizes template nanoparticles in which two or more of their atoms can be oxidized by one metal ion, which is reduced at the expense of the template atoms. By the galvanic replacement technique, new metallic nanocages have been made, such as PtNCs<sup>22,23</sup> and PdNCs,<sup>23,24</sup> as well as shell–shell hollow nanoparticles made of different shells, for example, gold–platinum (AuPtNCs),<sup>9</sup> platinum–palladium (PtPdNCs),<sup>22,23</sup> and palladium–platinum (PdPtNCs).<sup>22,23</sup> Several requirements that should be considered

in the galvanic replacement technique have been mentioned in details in our previous article.<sup>22</sup>

We have used silver nanocubes (AgNCs) as a template for the synthesis of both single shell metal nanoreactors<sup>31</sup> (e.g., AuNCs,<sup>19</sup> PtNCs,<sup>22,23</sup> and PdNCs<sup>22,23</sup>) and shell–shell double metal nanoreactors (e.g., AuPdNCs, AuPtNCs, PtPdNCs, and PdPtNCs).<sup>22,23</sup> Figure 6A shows the TEM image of PtNCs prepared by the galvanic replacement of silver atoms within the AgNC template by platinum, while Figure 6B is the high-resolution TEM image of the PtNCs in Figure 6A. The PtPdNCs shell–shell nanoreactor was prepared also from a AgNC template.<sup>22,23</sup> Figure 6C,D shows the high-resolution TEM of PtPdNCs.<sup>22</sup> Figure 7 shows AuPtNC<sup>9</sup> and AuPdNC<sup>9,22</sup> shell–shell nanoparticles. The advantage of the AuPtNC and AuPdNC shell–shell nanoreactor is that they have a localized surface plasmon resonance (LSPR) in addition to a catalytically active surface.<sup>9,22</sup> The scanning transmission electron microscopy coupled with X-ray energy dispersive microanalysis (STEM-XEDS) were successfully used to image the distribution of the elements present on the outer surface of the shell–shell nanoparticles.<sup>9</sup> Figure 7A,C shows the TEM images of AuPtNCs and AuPdNCs, while a magnified SEM image of AuPdNCs is shown in Figure 7D. Figure 7B shows

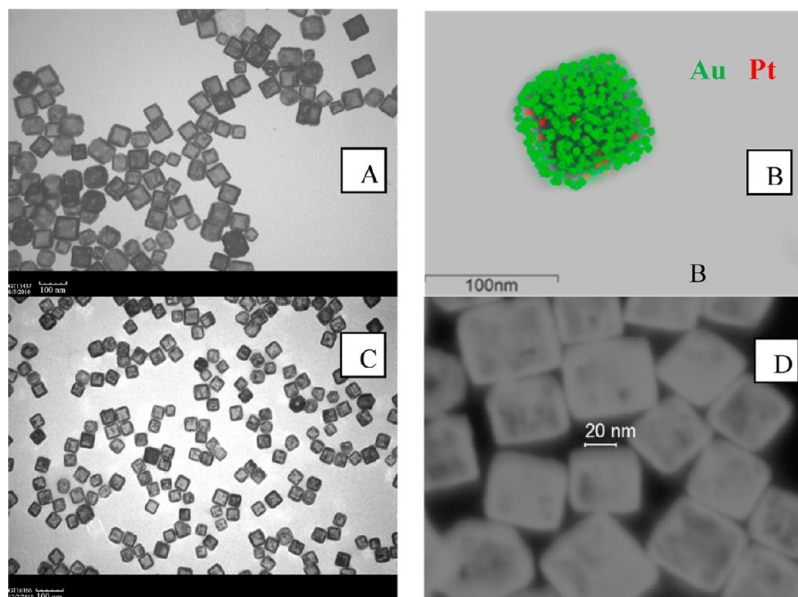


**FIGURE 7.** (A) TEM image of AuPtNCs. (B) STEM-XEDS elemental map imaging of AuPtNCs. (C) TEM of AuPdNCs shell-shell nanoreactors. (D) Magnified-SEM image of AuPdNC shell-shell nanoreactors.

aSTEM-XEDS map of AuPdNCs shell-shell nanoreactor. It is clear that the outer surface is made of gold atoms and the Pt atoms are present in the pores and under the layer of gold.<sup>9</sup>

**3.3. Catalysis by Hollow Nanoparticles Occurring in the Cage (Cage Effect): The Different Experiments.** In order to conduct catalysis with nanocages and to study the cage effect in nanocatalysis with hollow nanoparticles, new metallic hollow nanoparticles have been prepared with one or two shell structures.<sup>9,22</sup> The synthesized hollow nanoparticles were used to examine the confinement effect of the reactants inside the cavity. Below, we discuss in detail the different experiments aimed at finding out whether the nanocatalysis is occurring on the interior or exterior surface of the nanoparticle.

**3.3.1. Comparing the Kinetic Parameters.** The nanoreactor cage effect in nanocatalysis has been studied by comparing kinetic parameters of a model reaction that can be catalyzed on the exterior and interior surface shells of the shell-shell hollow nanoreactors.<sup>23</sup> Six hollow nanoparticles of different compositions were used to conduct a comparative kinetic study. These were following nanocages: PtNCs, PdNCs, PtPdNCs, PdPtNCs, AuPtNCs, and Pt-Pd alloy.<sup>23</sup> The kinetic parameters (rate constants, activation energies, frequency factors, and entropies of activation) of the reduction of 4-nitrophenol (4NP) with sodium borohydride (SBH) were determined when the same concentrations of these nanocatalysts is used.<sup>22,23</sup> The values of the kinetic parameters of PdNCs and PtPdNCs (which has the inner shell made of Pd)

were comparable.<sup>26,27</sup> Similarly, the kinetic parameters for the catalysis of the same reaction by PtNCs and PdPtNCs shell-shell (in which the inner shell was made of Pt)<sup>22</sup> were similar (see Table 1). This suggests that the catalytic reaction took place in the cavity of the nanocages and was catalyzed by the inner surface. In addition to the similarity of the values of the kinetic parameters, as a result of the nanoreactor confinement effect of the hollow nanocatalysts, the frequency factors obtained from the Arrhenius plots were found to be the highest ever reported for this reduction reaction (see Table 1). This might be due to the confinement effects.<sup>9,23</sup>

In the case of catalysis with AuPtNCs, in which gold was on the outer shell instead of Pd, the activation energy was higher than that when PdPtNCs were used.<sup>9</sup> This observed change in the activity of the platinum covered by gold might suggest the coparticipation in the catalysis of the outer shells. There are at least two possible kinds of coparticipations. In one, the reaction can be catalyzed by both the inside and outside surfaces with different contributions but with dominance of the inside surface catalysis. The other could be that the catalysis is occurring on the inside surface but the electron pool on the inside surface has a contribution from the exterior surface (the gold). There are two observations favoring this proposal: First, the fact that the rate constant is an order of magnitude larger than others could be a reflection of the fact that gold is generous with its electrons. Second, the fact that the frequency factor of the catalysis

**TABLE 1.** Comparison of Kinetic Parameters of 4NP with SBH When Catalyzed with Pt–Pd Alloy NCs, PdNCs, PtPdNCs, PdPtNCs, and PtNCs<sup>23</sup>

nanocatalyst	rate constant at 25 °C (min <sup>-1</sup> )	activation energy (kcal/mol)	entropy of activation (cal/(mol·K))	frequency factor (min <sup>-1</sup> )
PtPd alloy NCs	0.0133 ± 1.1 × 10 <sup>-4</sup>	26.2 ± 1.8	79.4 ± 6.0	1.76 × 10 <sup>17</sup>
PdNCs	0.0190 ± 8.7 × 10 <sup>-4</sup>	22.6 ± 1.5	67.8 ± 5.0	5.10 × 10 <sup>14</sup>
PtPdNCs	0.0035 ± 1.3 × 10 <sup>-4</sup>	20.7 ± 1.8	61.4 ± 6.0	2.13 × 10 <sup>13</sup>
PdPtNCs	0.0190 ± 2.0 × 10 <sup>-4</sup>	18.5 ± 1.3	50.4 ± 4.2	8.80 × 10 <sup>9</sup>
PtNCs	0.0036 ± 2.0 × 10 <sup>-4</sup>	16.2 ± 1.1	43.2 ± 3.6	2.31 × 10 <sup>9</sup>
AuPtNCs	0.0190 ± 1.0 × 10 <sup>-3</sup>	21.0 ± 0.6	63.6 ± 1.8	3.5 × 10 <sup>13</sup>

with AuPtNCs is very high could point to the presence of confinement and thus cavity catalysis.<sup>9</sup> There is a third possible scenario, which is this observation could result from a difference in the interface and the crystal and phonon structure of a thin layer of both metals or an alloy formed from the thin layers of two different metals made by this technique. This is very hard to calculate or predict at this time.

**3.3.2. Using the Plasmonic Effect.** When plasmonic nanoparticles are exposed to light of resonance frequency, their free conduction band electrons oscillate collectively giving rise to localized surface plasmon resonance (LSPR) that has a very strong extinction band. The LSPR peak shifts when the dielectric constant of the surrounding medium is changed. This optical property of the plasmonic nanoparticles can thus be used in sensing the changes in the chemical composition<sup>9</sup> (like that occurring during a chemical reaction) at the surface of the gold or silver nanocatalyst. Below, we shall use this important property. By placing the gold shell inside (in the cage) or outside, we can determine which surface causes changes in its chemical environment due to its catalytic activity.<sup>9</sup>

Gold nanocages (AuNCs) are characterized by the presence of two surfaces (inner and outer) and thus two plasmon fields.<sup>21</sup> When the dielectric constant of the medium changes around the outer surface only, the LSPR shifts to a different extent from that observed when the dielectric constant of the medium changes around both surfaces. Two types of nanoreactors were used in order to prove the cage effect using the change in the dielectric constant; one had a single shell (AuNCs) nanocage (with two plasmonic surfaces) and the other had double shell hollow nanoparticle<sup>9</sup> with an external plasmonic gold shell and a platinum internal shell (AuPtNCs).<sup>9</sup> The reduction reaction of 4NP with SBH is thus used to test for the cage effect by using AuNC and AuPtNC hollow nanoparticles. The changes in the peak position of the LSPR of the nanocatalyst were studied right after the addition of the reactants and during the course of the reaction. From the time dependence of the LSPR peak shift, resulting from the addition and during the course of this

catalytic reaction by using AuNCs or AuPtNCs; it was concluded that the catalysis is taking place within the cavity of the two nanocatalysts for the following observations: (1) Two sequential LSPR peak shifts; an immediate one followed by another one later in time, were observed for the AuNC nanoparticles, while a single rapid shift for AuPtNC nanoparticles was noted.<sup>9</sup> This is consistent with the presence of two plasmonic surfaces for the AuNCs but only one for AuPtNCs.<sup>9</sup> The time delay of the second shift and the induction period in the AuNC kinetics suggests that the solution of the reactants takes time to diffuse and be adsorbed on the inner gold surface to react or to form the rate-determining intermediate species.<sup>9</sup> (2) The observed shift in the LSPR is blue suggesting that the adsorbed species or its products change the surrounding medium to one of lower dielectric constant. That is to say, SBH is first adsorbed and decomposed giving H<sub>2</sub> gas.<sup>9</sup> (3) There is an observed induction period for the reaction to begin and after the observation of the initial plasmon shift. This suggests that the shift is determined by the rate of diffusion of the reaction mixture to the surface and its displacement of the old medium. After the mixture reaches the surface, the reaction's rate is determined by the slow rate-determining step of the reaction. (4) The observation of an induction period in the two nanoreactors suggests that catalysis occurs in the inner cavity surface of the hollow nanoparticles. This is further supported by the observation that the reaction's activation energy is ~7 kcal/mol for AuNCs but ~21 kcal/mol for AuPtNCs, which have thick Pt interior walls.<sup>9</sup> Figure 8A,B shows the LSPR spectra of pure AuNCs and of AuPtNCs, respectively, after mixing with pure 4NP, pure BH, and a mixture of 4NP and BH at 0 min and 30 min from mixing. The amount of the shift in the LSPR is given in Table 2.

**3.3.3. Rate Dependence on Holes in the Cage.** It is known that methyl orange dye (MO) can be photodegraded in the presence of semiconductors, for example, TiO<sub>2</sub>, ZnO<sub>2</sub>, or Ag<sub>2</sub>O. AuNCs were made by the galvanic replacement method<sup>22</sup> but with the incomplete removal of the inner Ag atoms inside the AuNCs; Ag is oxidized to silver oxide (Ag<sub>2</sub>O)



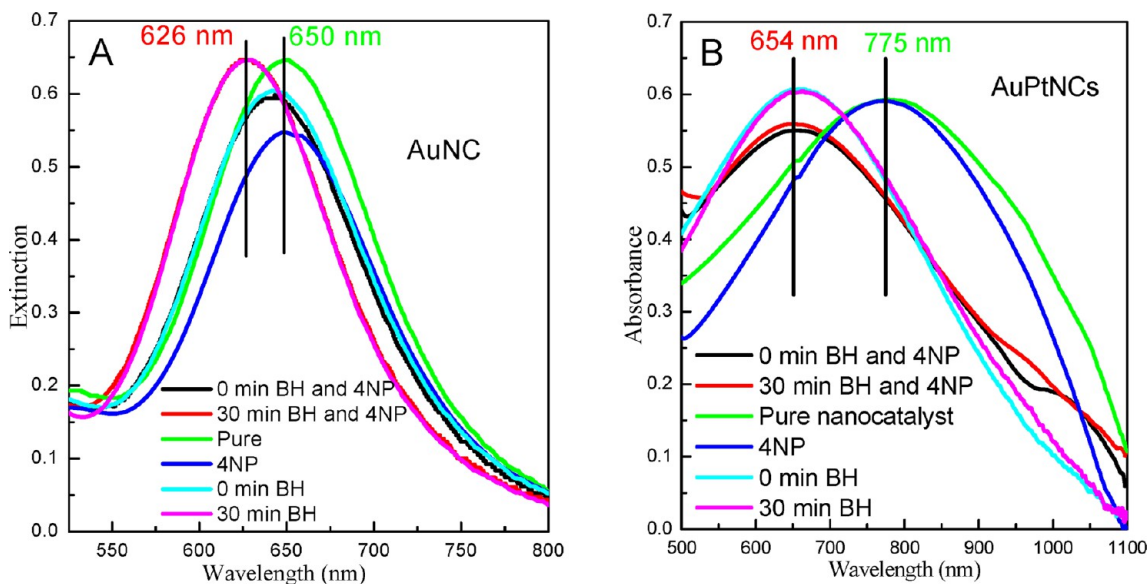


**FIGURE 8.** The time dependence of the reduction reaction between sodium borohydride (SBH) and 4-nitrophenol (4NP) catalyzed by AuNCs (A) and AuPtNCs (B) and followed by the shift in the localized surface plasmon resonance (LSPR) spectra of these catalysts.<sup>9</sup>

**TABLE 2.** Summary of the LSPR Peak Position for AuNCs and AuPtNCs before and after Mixing with the 4NP and SBH<sup>a9</sup>

	LSPR before mixing (nm)	LSPR immediately after mixing of BH and 4NP (nm)	LSPR after 30 min from mixing BH and 4NP (nm)	LSPR blue shift right after mixing (nm)	LSPR blue shift 30 min (nm)
AuNCs	650	642	626	8	24
AuPtNCs	775	654	654	121	121

<sup>a9</sup>The fifth and sixth columns give the amount of shift in the LSPR peak position compared with those for the pure nanoparticles at 0 and 30 min, respectively.

semiconductor upon exposure to dissolved O<sub>2</sub> in the water solvent (Figure 8A).<sup>20</sup> The excitation of Ag<sub>2</sub>O oxidizes the water molecules into hydroxyl radicals, which destroy the MO molecules and bleach its color (Figure 8B).<sup>20</sup> The rate of reaction, followed optically, is then studied as a function of the size and the number of the holes on the cage walls. If the reaction occurs inside the cavity, then there will an optimum number or size of the holes on the wall due to the confinement of the radicals within the cage. This was indeed observed. The rate first increased and then decreased as the size or the number of the holes increases (Figure 9C).

#### 4. Some Comments on Nanocatalysis in Solution

In this field, the important question whether catalytic reaction occurs on the metal surface or in solution has not yet been answered. In this Account, we have given a few examples of catalytic reactions that suggested that solid nanoparticles with rough surfaces and hollow ones with the appropriate number and size of holes on their walls can be efficient nanocatalysts. The cause of the catalytic activity in the solid ones is the fact that atoms at these positions do

not have the full number of chemical bonds that satisfy their chemical valency.

The reason for the catalytic activity of the hollow nanoparticles could be the confinement (cage) effect of the cavity that could build up the concentration of the species involved in the rate-determining step. Another possible reason could be the presence of less capping material on the inner surface than the external surface.

We do not want in any way to generalize the above conclusions, even though a number of publications by other workers have appeared in the literature confirming the rough surface and the confinement effects causing catalytic enhancement. If this is the case, one may conclude that the best catalysts are made with many nanoscale cavities having rough surfaces.

There are other properties that can be important in increasing the performance of nanocatalysts and enhancing their selectivity. The design of the nanocatalyst has to be made to sustain high chemical activity, high surface area, high degree of roughness, less capping materials, and hollow structure having suitable cavity size with the appropriate number and size of the hole on its walls. The metal atom

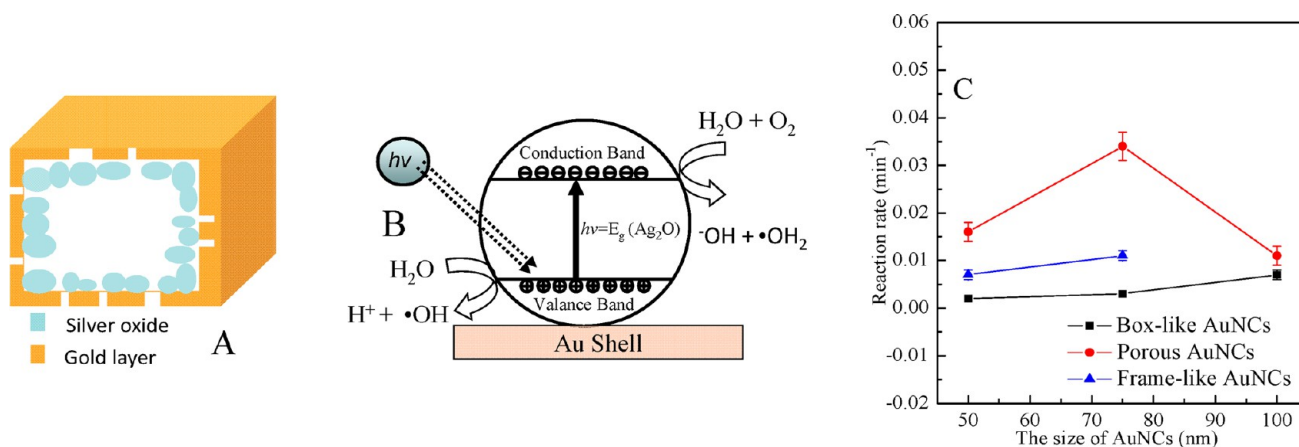


**FIGURE 9.** (A) Schematic diagram of gold nanocage with a layer of silver oxide on the inside surface resulting from the oxidation of the remaining Ag layer in the synthesis of the gold nanocage from silver cubes. (B) The mechanism of photocatalyzed formation of the OH radicals by silver oxide and water inside the AuNC nanoreactor. (C) The effect of the hole size of AuNCs and pore numbers and sizes and the photodegradation rate constant.<sup>20</sup>

diffusion between the two shells in the two shell hollow nanoparticles could lead to changes in the structure and the catalytic properties of these nanoparticles during the reaction and especially at high temperatures. This could interfere with determining activation energy. The effect of the shell thicknesses of shell–shell nanocatalyst on the catalytic properties has to be determined in the future. The degree of cleanness of the inner surface of the hollow nanocatalyst needs to be studied. The synthesis of these nanoparticles is critical. We thus encourage work in this field to be accompanied by careful characterization of the hollow nanoparticles using different imaging techniques.

*This work is supported by the National Science Foundation (Grant No. 0957335). We acknowledge Justin Bordley for his careful and critical reading of this Account.*

#### BIOGRAPHICAL INFORMATION

**Mahmoud A. Mahmoud** joined the Laser Dynamics Laboratory, Georgia Tech, in 2007 as a Postdoctoral Associate and later as a Research Scientist II under the direction of Prof. Mostafa A. El-Sayed. Since 2004, he has published over 50 peer-reviewed papers. He received his B.S. degree in chemistry from Zagazig University and M.S. degree in physical chemistry from the National Institute of Laser Enhanced Sciences (NILES) at Cairo University, Egypt, in ultrafast spectroscopic and dynamical studies of the photofragmentation of carbonyl compounds. In 2007, he received his Ph.D. in physical and inorganic chemistry from the NILES in optical, biological, and catalytic properties of nanoparticles.

**Radha Narayanan** received her B.S. in chemistry from Armstrong Atlantic State University in Savannah, Georgia, in May 2000. She then pursued her graduate studies in analytical chemistry under the direction of Professor Mostafa A. El-Sayed and obtained her Ph.D. from Georgia Tech in May 2005. She then

conducted her postdoctoral studies under Professor Marc D. Porter at the University of Utah. She is currently an Assistant Professor of Chemistry at the chemistry department at the University of Rhode Island. She is currently managing a group of 10 graduate and undergraduate students in nanosensor and nanocatalysis research.

**Mostafa A. El-Sayed** is Regents' Professor and Julius Brown Chair in the School of Chemistry and Biochemistry at Georgia Tech. He obtained his Ph.D. from Florida State University in 1959 with Michael Kasha, and after postdoctoral fellowships at Harvard, Yale, and Caltech, he joined the faculty at UCLA in 1961 and Georgia Tech later in 1994. He is currently an elected member of the U.S. National Academy of Science, an elected fellow of the American Academy of Arts and Sciences, former editor-in-chief of the *Journal of Physical Chemistry*, and recipient of the Ahmed Zewail prize in molecular sciences, the ACS Irving Langmuir Prize in Chemical Physics, the Glenn T. Seaborg Medal, and the U.S. National Medal of Science. El-Sayed's laboratory is consistently ranked among the top chemical research laboratories of the past decade, no. 4 worldwide in 2009 by Times Higher Education.

#### FOOTNOTES

\*E-mail: melsayed@gatech.edu.

The authors declare no competing financial interest.

#### REFERENCES

- Freund, P. L.; Spiro, M. Colloidal catalysis: The effect of sol size and concentration. *J. Phys. Chem.* **1985**, *89*, 1074–1077.
- Ahmadi, T. S.; Wang, Z. L.; Green, T. C.; Henglein, A.; El-Sayed, M. A. Shape-controlled synthesis of colloidal platinum nanoparticles. *Science* **1996**, *272*, 1924–1926.
- Narayanan, R.; El-Sayed, M. A. Shape-dependent catalytic activity of platinum nanoparticles in colloidal solution. *Nano Lett.* **2004**, *4*, 1343–1348.
- Narayanan, R.; El-Sayed, M. A. Effect of colloidal nanocatalysis on the metallic nanoparticle shape: The Suzuki reaction. *Langmuir* **2005**, *21*, 2027–2033.
- Eppler, A.; Ruppel, G.; Gucci, L.; Somorjai, G. A. Model catalysts fabricated using electron beam lithography and pulsed laser deposition. *J. Phys. Chem. B* **1997**, *101*, 9973–9977.
- Narayanan, R.; El-Sayed, M. A. Changing catalytic activity during colloidal platinum nanocatalysis due to shape changes: Electron-transfer reaction. *J. Am. Chem. Soc.* **2004**, *126*, 7194–7195.

- 7 Mahmoud, M. A.; Tabor, C. E.; El-Sayed, M. A.; Ding, Y.; Wang, Z. L. A new catalytically active colloidal platinum nanocatalyst: The multiarmed nanostar single crystal. *J. Am. Chem. Soc.* **2008**, *130*, 4590–4591.
- 8 Lee, I.; Zaera, F. Catalytic conversion of olefins on supported cubic platinum nanoparticles: Selectivity of (100) versus (111) surfaces. *J. Catal.* **2010**, *269*, 359–366.
- 9 Mahmoud, M. A.; El-Sayed, M. A. Time dependence and signs of the shift of the surface plasmon resonance frequency in nanocages elucidate the nanocatalysis mechanism in hollow nanoparticles. *Nano Lett.* **2011**, *11*, 946–953.
- 10 Narayanan, R.; El-Sayed, M. A. Effect of colloidal catalysis on the nanoparticle size distribution: Dendrimer-Pd vs PVP-Pd nanoparticles catalyzing the Suzuki coupling reaction. *J. Phys. Chem. B* **2004**, *108*, 8572–8580.
- 11 Borodko, Y.; Habas, S. E.; Koebel, M.; Yang, P. D.; Frei, H.; Somorjai, G. A. Probing the interaction of poly(vinylpyrrolidone) with platinum nanocrystals by UV-Raman and FTIR. *J. Phys. Chem. B* **2006**, *110*, 23052–23059.
- 12 Zhao, H.; Yin, F.-J.; Xu, X.-Y.; Tong, Z.; Zheng, J.-W.; Zhao, G. A novel catalyst SiO<sub>2</sub>@NiO for reduction of 4-NP. *Synth. React. Inorg., Met.-Org., Nano-Met. Chem.* **2007**, *37*, 15–18.
- 13 Witham, C. A.; Huang, W. Y.; Tsung, C. K.; Kuhn, J. N.; Somorjai, G. A.; Toste, F. D. Converting homogeneous to heterogeneous in electrophilic catalysis using monodisperse metal nanoparticles. *Nat. Chem.* **2010**, *2*, 36–41.
- 14 Sun, Y. G.; Mayers, B.; Xia, Y. N. Metal nanostructures with hollow interiors. *Adv. Mater.* **2003**, *15*, 641–646.
- 15 Mahmoud, M. A.; El-Sayed, M. A. Aggregation of gold nanoframes reduces, rather than enhances, SERS efficiency due to the trade-off of the inter- and intraparticle plasmonic fields. *Nano Lett.* **2009**, *9*, 3025–3031.
- 16 Grunes, J.; Zhu, A.; Somorjai, G. A. Catalysis and nanoscience. *Chem. Commun.* **2003**, 2257–2260.
- 17 Narayanan, R.; El-Sayed, M. A. Effect of nanocatalysis in colloidal solution on the tetrahedral and cubic nanoparticle shape: Electron-transfer reaction catalyzed by platinum nanoparticles. *J. Phys. Chem. B* **2004**, *108*, 5726–5733.
- 18 Sun, Y. G.; Xia, Y. N. Shape-controlled synthesis of gold and silver nanoparticles. *Science* **2002**, *298*, 2176–2179.
- 19 Mahmoud, M. A.; El-Sayed, M. A. Comparative study of the assemblies and the resulting plasmon fields of Langmuir-Blodgett assembled monolayers of silver nanocubes and gold nanocages. *J. Phys. Chem. C* **2008**, *112*, 14618–14625.
- 20 Yen, C. W.; Mahmoud, M. A.; El-Sayed, M. A. Photocatalysis in gold nanocage nanoreactors. *J. Phys. Chem. A* **2009**, *113*, 4340–4345.
- 21 Mahmoud, M. A.; Snyder, B.; El-Sayed, M. A. Surface plasmon fields and coupling in the hollow gold nanoparticles and surface-enhanced Raman spectroscopy. Theory and experiment. *J. Phys. Chem. C* **2010**, *114*, 7436–7443.
- 22 Mahmoud, M. A.; El-Sayed, M. A. Metallic double shell nanocages: The challenges of their synthetic techniques. *Langmuir* **2012**, *28*, 4051–4059.
- 23 Mahmoud, M. A.; Saira, F.; El-Sayed, M. A. Experimental evidence for the nanocage effect in catalysis with hollow nanoparticles. *Nano Lett.* **2010**, *10*, 3764–3769.
- 24 Macdonald, J. E.; Bar Sadan, M.; Houben, L.; Popov, I.; Banin, U. Hybrid nanoscale inorganic cages. *Nat. Mater.* **2010**, *9*, 810–815.
- 25 Gonzalez, E.; Arbiol, J.; Puntès, V. F. Carving at the nanoscale: Sequential galvanic exchange and Kirkendall growth at room temperature. *Science* **2011**, *334*, 1377–1380.
- 26 Lim, B. W.; Lu, X. M.; Jiang, M. J.; Camargo, P. H. C.; Cho, E. C.; Lee, E. P.; Xia, Y. N. Facile synthesis of highly faceted multioctahedral Pt nanocrystals through controlled overgrowth. *Nano Lett.* **2008**, *8*, 4043–4047.
- 27 Narayanan, R.; El-Sayed, M. A. Changing catalytic activity during colloidal platinum nanocatalysis due to shape changes: Electron-transfer reaction. *J. Am. Chem. Soc.* **2004**, *126*, 7194–7195.
- 28 Li, Y.; Hong, X. M.; Collard, D. M.; El-Sayed, M. A. Suzuki cross-coupling reactions catalyzed by palladium nanoparticles in aqueous solution. *Org. Lett.* **2000**, *2*, 2385–2388.
- 29 Zeng, J.; Zhang, Q.; Chen, J. Y.; Xia, Y. N. A comparison study of the catalytic properties of Au-based nanocages, nanoboxes, and nanoparticles. *Nano Lett.* **2010**, *10*, 30–35.
- 30 Eddaoudi, M.; Kim, J.; Rosi, N.; Vodak, D.; Wachter, J.; O’Keeffe, M.; Yaghi, O. M. Systematic design of pore size and functionality in isorecticular MOFs and their application in methane storage. *Science* **2002**, *295*, 469–472.
- 31 Graeser, M.; Pippel, E.; Greiner, A.; Wendorff, J. H. Polymer core-shell fibers with metal nanoparticles as nanoreactor for catalysis. *Macromolecules* **2007**, *40*, 6032–6039.
- 32 Park, J. C.; Bang, J. U.; Lee, J.; Ko, C. H.; Song, H. Ni@SiO<sub>2</sub> yolk-shell nanoreactor catalysts: High temperature stability and recyclability. *J. Mater. Chem.* **2010**, *20*, 1239–1246.
- 33 Peng, Z. M.; You, H. J.; Wu, J. B.; Yang, H. Electrochemical synthesis and catalytic property of sub-10 nm platinum cubic nanoboxes. *Nano Lett.* **2010**, *10*, 1492–1496.
- 34 Yadav, M.; Akita, T.; Tsumori, N.; Xu, Q. Strong metal-molecular support interaction (SMMSI): Amine-functionalized gold nanoparticles encapsulated in silica nanospheres highly active for catalytic decomposition of formic acid. *J. Mater. Chem.* **2012**, *22*, 12582–12586.
- 35 Snyder, J.; McCue, I.; Livi, K.; Erlebacher, J. Structure/processing/properties relationships in nanoporous nanoparticles as applied to catalysis of the cathodic oxygen reduction reaction. *J. Am. Chem. Soc.* **2012**, *134*, 8633–8645.
- 36 Hong, J. W.; Kang, S. W.; Choi, B. S.; Kim, D.; Lee, S. B.; Han, S. W. Controlled synthesis of Pd–Pt alloy hollow nanostructures with enhanced catalytic activities for oxygen reduction. *ACS Nano* **2012**, *6*, 2410–2419.
- 37 de la Hoz, J. M. M.; Balbuena, P. B. Geometric and electronic confinement effects on catalysis. *J. Phys. Chem. C* **2011**, *115*, 21324–21333.
- 38 Caruso, F.; Caruso, R. A.; Mohwald, H. Nanoengineering of inorganic and hybrid hollow spheres by colloidal templating. *Science* **1998**, *282*, 1111–1114.
- 39 Yin, Y. D.; Rioux, R. M.; Erdonmez, C. K.; Hughes, S.; Somorjai, G. A.; Alivisatos, A. P. Formation of hollow nanocrystals through the nanoscale Kirkendall effect. *Science* **2004**, *304*, 711–714.